Technology and Science for the Ships of the Future
V. Crupi and V. Bucci (Eds.)

doi:10.3233/PMST250119

Experimental Techniques for the Assessment of the Mechanical Behaviour of HDPE Used in Boat Building

Giuseppe Brando[1,a], Serena Bertagna[b], Vincenzo Crupi[a], Fabio Distefano[a], Gabriella Epasto[a], Alberto Marinò[b]
[a]*Department of Engineering, University of Messina, 98166 Messina, Italy*
[b]*Department of Engineering and Architecture, University of Trieste, 34127 Trieste, Italy*
Giuseppe Brando https://orcid.org/0009-0005-9173-7810
Serena Bertagna https://orcid.org/0000-0002-1100-5048
Vincenzo Crupi https://orcid.org/0000-0001-7498-4733
Fabio Distefano https://orcid.org/0000-0002-0255-5857
Gabriella Epasto https://orcid.org/ 0000-0003-1372-5871
Alberto Marinò https://orcid.org/0000-0001-7498-4733

Abstract. High-performance polymeric materials, such as high-density polyethylene (HDPE), can be considered a good choice for building boat hulls. HDPE is a thermoplastic polymer; hence, it has the advantage of being recycled and easy to produce. Moreover, its high corrosion and chemical resistance makes this material suitable for the marine environment. The application of HDPE in boatbuilding is relatively new. Thus, a deep knowledge of its mechanical properties as well as failure modes under mechanical loads is required. Preliminarily, non-destructive evaluation of defects due to the production technology has been performed on the HDPE specimens by active thermography and ultrasonic phased array. The mechanical behaviour under different loading conditions (tensile, bending) has been experimentally evaluated. The strain field during tensile tests has been calculated by digital image correlation technique and thermal behaviour was detected by infrared thermography. The experimental campaign aimed at assessing the mechanical strength of the investigated HDPE material. The effect of strain rate on their mechanical behaviour was also evaluated. For this reason, the specimens were subjected to different test speed. The results of mechanical tests highlighted that HDPE has good mechanical properties and very high ductility, together with the ability to give highly concentrated deformation (necking) and fibrillar failure.

Keywords: ship structures and materials; high-density polyethylene; boat hulls; mechanical properties; experimental techniques.

1. Introduction

Fiber Reinforced Plastic (FRP) boats currently make up 90% of the circulating boats, despite the high level of pollution resulting from their production and disposal, so they represent a significant problem for the environment and related health issues [1, 2].

[1] Corresponding Author: Giuseppe Brando, giuseppe.brando@studenti.unime.it

The adoption of eco-friendly materials, such as wood [3,4], and disruptive technologies, such as additive manufacturing, leads to obtain both a sustainable ship life-cycle and a weight reduction in accordance with the Green Shipbuilding approach [5-7]. In this context, there is a lot of attention towards plastic materials derived from recycled material. Specifically, high-density polyethylene (HDPE), a thermoplastic polymer belonging to the polyolefin family, is finding wide application in the nautical field as a structural material for the construction of small-size vessels [8, 9], with specific reference to workboats. HDPE is a durable material, which combines chemical resistance and anti-corrosion properties, so it is well suited for long-term use. From the environmental point of view, HDPE is recyclable in all its forms, despite being derived from petroleum, and can be recycled into filaments for Additive Manufacturing (AM) technology or chipped material for use in thermoforming processes such as rotational moulding [10, 11]. Furthermore, the same HDPE material, usable in the nautical field, can be produced from virgin material and/or recycled material [12, 13], so HDPE is perfect for inclusion in a circular economy process. In terms of processing approaches, its thermoplastic nature guarantees high ease of working and the possibilities of shaping it to achieve complex and specifically designed geometries. As regards mechanical properties, HDPE is characterised by high impact resistance, wear resistance, stiffness, corrosion, and chemical resistance. In addition, it benefits from high electrical resistance, acting as an insulator that blocks electricity and heat, and the capacity of not absorbing moisture. Other important properties are non-toxicity and long-life cycle. The basic structural elements come in two forms: “single skin” panels and sandwich panels, made of two thin skins with a HDPE honeycomb core, which are particularly interesting for the construction of boat superstructures, as they can offer self-supporting characteristics in terms of structure and thermal-acoustic insulation.

Within boatbuilding applications, the lower density of HDPE with respect to water enhances the buoyancy capacity of vessels and allows for an increase of the maximum payload. In addition, HDPE boats have a good resistance to marine growth: anti-fouling coatings are not necessary, with important benefits for the surrounding environment. Its toughness and durability enable withstanding impact from collisions with debris, rocks, or other vessels, reducing the risk of damage and subsequent repairs. Finally, HDPE no-ageing property and UV-ray resistance, durability, and low maintenance requirements may result in a significant reduction of operational costs. On the other hand, the biggest disadvantages of HDPE are its higher market cost, compared to traditional composites used in boat building, and the current limited expertise about this material.

Knowledge of the quality and mechanical properties of HDPE is of extreme significance for its application in the nautical field. The Italian Ship Classification Society “Registro Italiano Navale (RINA)”, along with the French Classification Society “Bureau Veritas (BV)”, has recently introduced tailored rules [14- 16] to address the use of this material and define the requirements necessary for the classification of hulls made of HDPE [17]. Given the above framework, this study explores the mechanical characteristics of HDPE material for nautical constructions through mechanical tests and two experimental techniques, which were applied by some of the authors for the investigation of materials and welded joints [18, 19]: infrared thermography (IRT) and Digital Image Correlation (DIC). Bending and tensile tests were carried out on HDPE specimens. The tensile tests were performed on the following different typologies of dog bone HDPE specimens in order to compare their mechanical properties in terms of Young’s modulus and tensile strength: virgin, recycled and butt-welded joints manufactured by means of 2 technologies.

2. Materials and Methods

The tensile and the three and four-point bending tests were carried out using an *Italsigma* servo-hydraulic testing machine equipped with a 25 kN load cell. The load cell is calibrated according to ISO 7500-1 in Class 1. The experimental set-up included the following experimental techniques: IRT and DIC, which were applied simultaneously during the tests. DIC techniques, with open source *2D DIC software Ncorr v1.2*, was used to calculate the field of displacements and strains during the tensile tests. A speckle pattern was painted on the specimen surface using gel coat spray. The tests were recorded with a super-macro lens at a resolution of 1280 x 720 pixels and an acquisition rate of 60 fps. The images were calibrated, considering the dimensions of the specimens, with a resolution of 0.18 mm/pixel for the tensile specimens and 0.3 mm/pixel for the bending specimens. *FLIR SC640* infrared (IR) camera, whose characteristics are reported in Table 1, was applied during the tests to monitor the surface temperature of the specimen. The other surface of the specimens was painted black for applying the IRT technique and the IR camera was calibrated considering the blackbody reference for the surface emissivity. The thermal images were acquired at 3.75 Hz and analysed using the FLIR *ResearchIR Max* software. The experimental set-ups for tensile and bending tests are shown in Figures 1 and 2, respectively. The tensile tests were performed at actuator speed of 10 mm/min except for the specimens VT15S _1 and RT10S_1 whose speeds were respectively 2 mm/min and 5 mm/min. Static three- and four-point bending tests were carried out at a deflection rate of 10 mm/min. The lower support span has a length of 280 mm (Figures 3 and 4). The higher support span for the 4 point bending tests has a length of 130 mm (Figure 4).

Table 1. Thermal camera characteristics.

IR resolution	640 x 480 pixels
Sensor	Microbolometer
Lens	IR, focal length 38 mm
Accuracy	± 2°C
Thermal sensitivity	30mK @ 30°C
Spectral range	7.5 – 13 μm

Figure 1. Experimental set up for tensile tests.

Figure 2. Experimental set up for bending tests.

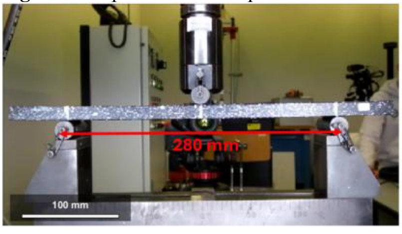

Figure 3. Three point bending test.

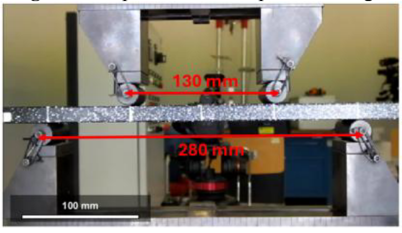

Figure 4. Four point bending test.

3. Results and discussion

3.1 Results of the bending tests on virgin HDPE specimens

The strain was evaluated during the bending tests by means of DIC analysis considering the deflection at the middle of the specimen on the lower surface. Figures 5 and 6 show the load-deflection curves of the four- and three-point bending tests, respectively. The bending tests were carried out on specimens having rectangular cross-section as shown in Figure 7. Figure 8 shows the specimen after the load removal. Figure 9 shows the DIC images detected during the bending test for VB15-9 specimen. The specimens were subjected to large deflection under bending loading (as shown in Figure 9) without fracture and a large amount of the deflection was recovered after the load was removed (Figure 8), confirming the deflection is mainly due to elastic strain.

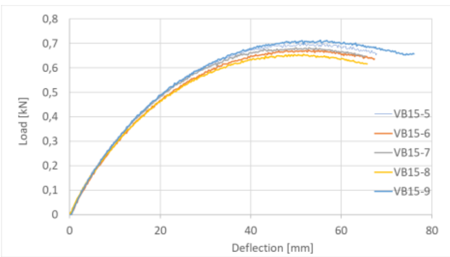

Figure 5. Load-deflection curves of the four-point bending tests.

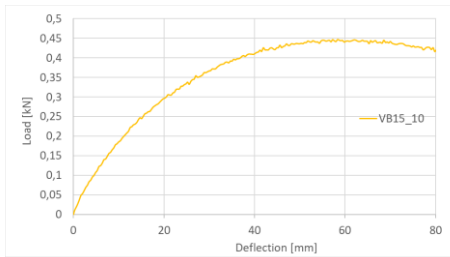

Figure 6. Load-deflection curves of the three-point bending tests.

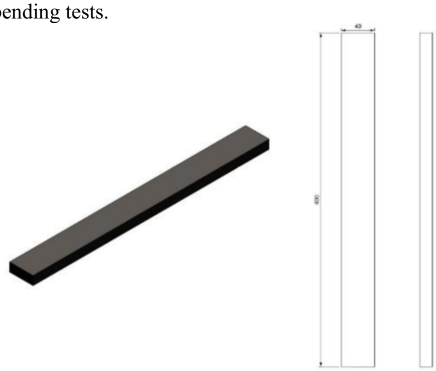

Figure 7. Geometry of the specimens for bending tests (t = 15 mm).

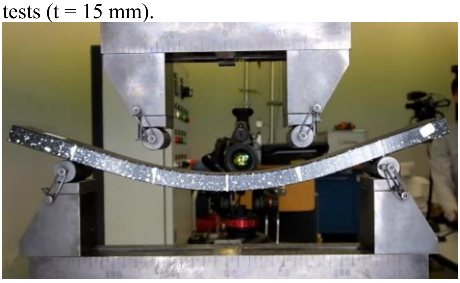

Figure 8. Specimen VB15-9 after load removal.

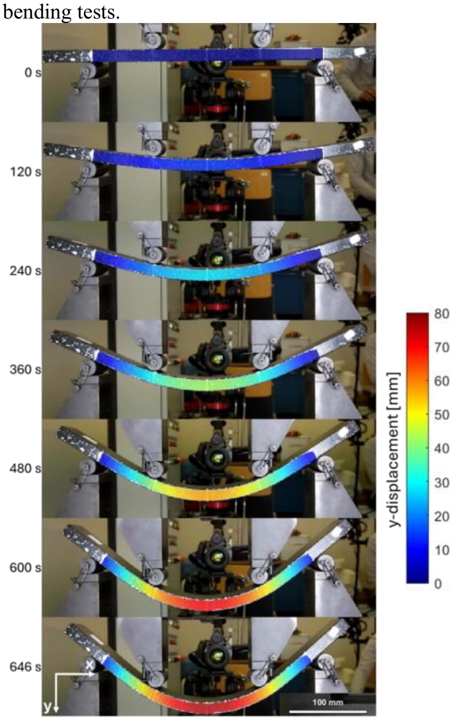

Figure 9. DIC images of the specimen VB15-9 during the bending test.

3.2 Results of the tensile tests on virgin and recycled HDPE specimens

The tensile tests were carried out on dog-bone virgin and recycled specimens (identified as VT15S and RT10S) with a geometry shown in Figure 11. The strain was evaluated during the tensile tests by means of DIC technique considering the displacement Δl respect to a reference length l_0 of 50 mm at the middle of the specimen (Figure 12). Figures 13 - 16 show the DIC and IRT images detected during the tensile tests for VT15S-2 and RT10S-2 specimens. Internal damage mechanics is the cause of the temperature increase in thermographic results. The VT15S and RT10S specimens were subjected to large permanent elongation under tensile loading (Figures 13 - 16) without fracture and the deformation was not recovered after the load was removed. Figures 17 and 18 show the load-displacement curves of the tensile tests for VT15S and RT10S specimens.

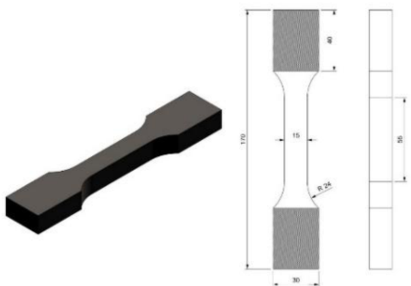

Figure 11. Geometry of the specimens for tensile tests.

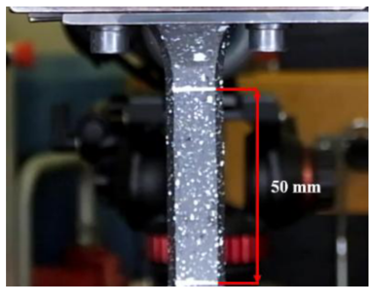

Figure 12. Reference length for the tensile tests.

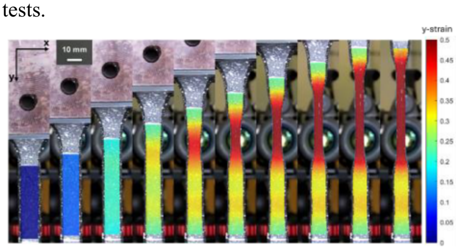

Figure 13. DIC images of the specimen VT15S - 2.

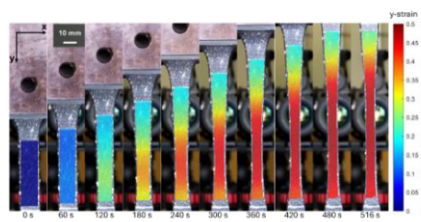

Figure 14. DIC images of the specimen RT10S - 2.

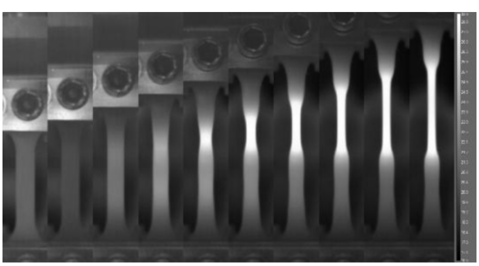

Figure 15. IRT image of the specimen VT15S_2

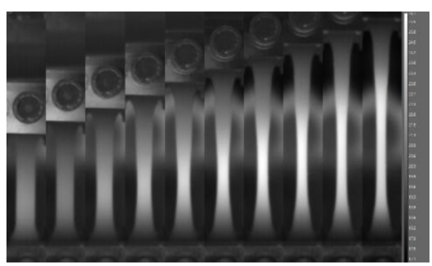

Figure 16. IRT image of the specimen RT10S_2

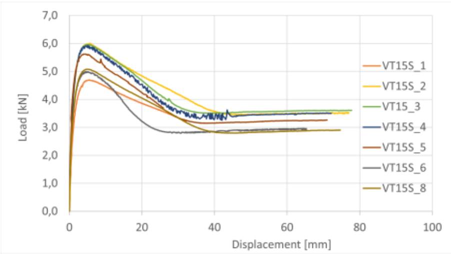

Figure 17. Load-displacement curves of the tensile tests for VT15S specimens.

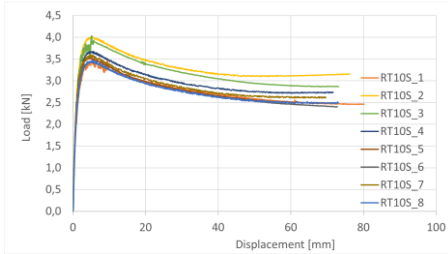

Figure 18. Load-displacement curves of the tensile tests for RT10S specimens.

The manufacturing of the welded specimens was based on the use of different equipment: a computer numerical control (CNC)-controlled automatic welding machine suitable for butt welding of plastic sheets (*TECNODUE* welding machine) and extrusion welding machine (*LEISTER FUSION 3C* extruder with *LEISTER TRIAC ST* heat gun). Some tensile tests were carried out on virgin HDPE butt welded dog-bone specimens, produced by means of machine welding with a thickness of 10 and 15 mm (identified as VT10BWM and VT15BWM) and extrusion welding with a thickness of 10 and 15 mm (identified as VT10BWE and VT15BWE). Figure 19 shows the geometry of the HDPE butt welded dog-bone specimens and some fractured specimens are shown in Figure 20. Figures 21 and 22 show the load-displacement curves of the tensile tests for VT10BWM and VT15BWM specimens. The VT10BWM specimens were subjected to large permanent elongation under tensile loading without fracture and the deformation was not recovered after the load was removed in a similar way to the VT15S specimens except for the VT10BWM-1 specimen which was subjected to fracture as can be seen from its load-displacement curve, which has a load drop (Figure 21). The VT15BWM specimens were subjected to fracture under tensile loading except for the VT15BWM-4 and VT15BWM-5 specimens which were not subjected to fracture as can be seen from their load-displacement curves, which have not a load drop (Figure 22).

Figures 23 and 24 show the load-displacement curves of the tensile tests for VT10BWE and VT15BWE specimens. The VT10BWE specimens were subjected to large permanent elongation under tensile loading without fracture and the deformation was not recovered after the load was removed in a similar way to the VT15S and VT10BWM specimens. The same response occurred for VT15BWE specimens except for the VT15BWE-4, VT15BWE-5 and VT15BWE-7 specimens which were subjected to fracture as can be seen from their curves, which have a load drop (Figure 24).

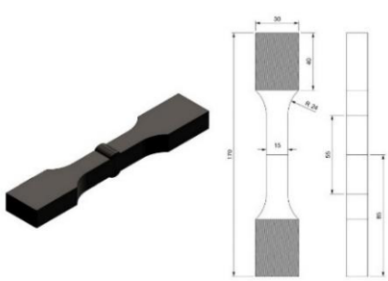

Figure 19. Geometry of the butt-welded dog-bone specimens for tensile tests.

Figure 20. Some specimens of different typologies fractured during the tensile tests: (a) VT15BWE_5, (b) VT15BWM_6, (c) VT10BWM_1.

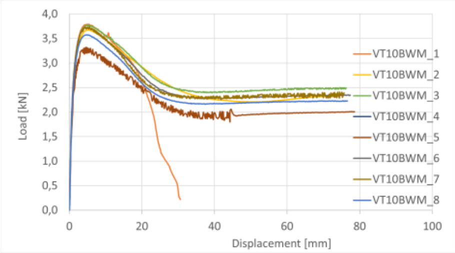

Figure 21. Load-displacement curves of the tensile tests for VT10BWM specimens.

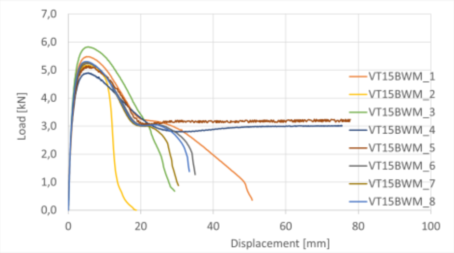

Figure 22. Load-displacement curves of the tensile tests for VT15BWM specimens.

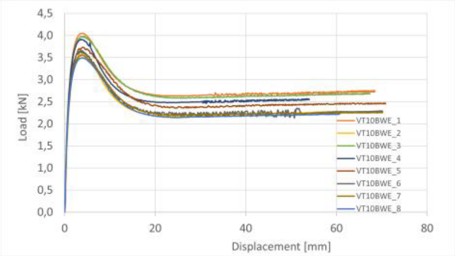

Figure 23. Load-displacement curves of the tensile tests for VT10BWE specimens.

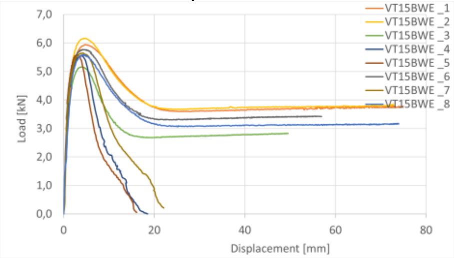

Figure 24. Load-displacement curves of the tensile tests for VT15BWE specimens.

Table 2 reports the average and standard deviation values of Young's Modulus and tensile strength, obtained by the tensile tests. The values of the Young's Modulus were evaluated by means of a *Matlab routine*. The value of Young's Modulus was considered equal to the slope of the linear curve, interpolating the stress-strain curve in order to achieve a value of the determination coefficient R^2=0.99. The low values of the standard deviation (Table 2) confirm that there is no high scattering between the tensile tests. The results of the tensile tests (Table 2) demonstrate that there is no significant difference between the mechanical properties of virgin and recycled HDPE and between the base material and the welded joints, obtained by two different welding manufacturing.

Table 2. Results for the tensile tests in terms of Young Modulus.

Specimen typology	Number of tested specimens	Average value of Young Modulus [MPa]	Standard deviation of Young Modulus [MPa]	Average value of tensile strength [MPa]	Standard deviation of tensile strength [MPa]
VT15S	7	943	68.1	24	2.3
RT10S	8	958	31.6	24	1.8
VT10BWM	8	1038	52.8	24	1.1
VT15BWM	8	931	64.3	24	1.2
VT10BWE	8	1119	78.7	25	1.5
VT15BWE	8	1060	45.5	25	1.2

4. Conclusions

Tensile and bending tests were performed on both virgin and recycled HDPE specimens and on welded joints. The experimental tests showed good repeatability. Regarding the bending test, it was observed that deformation was primarily due to elastic deformation. In the tensile test, the virgin and recycled HDPE specimens were subjected to significant permanent elongation under load without fracture, and the deformation was not recovered after load removal. A similar behavior was observed for the butt-welding dog-bone specimens (machine welding) VT10BWM and the butt-welded dog-bone specimens (extrusion welding) VT10BWE and VT15BWE, except for some specimens that fractured. Conversely, the VT15BWM dog-bone specimens predominantly fractured. From the tensile tests, it can be seen that there is no significant difference between the mechanical properties of the different typologies (virgin and recycled HDPE, base material and welded joints). In conclusion, virgin and recycled HDPE materials show promising mechanical properties for structural applications for boat building.

Acknowledgment

This study was carried out within the consortium iNEST (Interconnected Nord-Est Innovation Ecosystem) funded by the European Union Next-GenerationEU (Piano Nazionale di Ripresa e Resilienza (PNRR)-Missione 4 Componente 2, Investimento 1.5—D.D. 1058 23/06/2022, ECS_00000043).

References

[1] Nasso C, La Monaca U, Bertagna S, Braidotti L, Mauro F., Trincas G, Marinó A, Bucci V. Integrated design of an eco-friendly wooden passenger craft for inland navigation. Int. Shipbuild. Prog. 2019; 66(1): 35–55, doi: 10.3233/ISP-180254.

[2] Vo Dong PA., Azzaro-Pantel C, Cadene AL. Economic and environmental assessment of recovery and disposal pathways for CFRP waste management. Resour. Conserv. Recycl. 2018; 133: 63–75, doi: 10.1016/j.resconrec.2018.01.024.

[3] Corigliano P, Crupi V, Epasto G, Guglielmino E, Maugeri N, Marinò A. Experimental and theoretical analyses of Iroko wood laminates. Compos. Pt. B-Eng. 2017; 112(1): 251-264, doi: 10.1016/j.compositesb.2016.12.049.

[4] Corigliano P, Crupi V, Bertagna S, Marinò A. Bio-based adhesives for wooden boatbuilding. J. Mar. Sci. Eng. 2021; 9(1): 1–18, doi: 10.3390/jmse9010028.

[5] Li J, Yi H, Zhang Y. Research on green shipbuilding and concurrent green ship design. Appl. Mech. Mater. 2011; 44–47: 614–618, 2011, doi: 10.4028/www.scientific.net/AMM.44-47.614.

[6] Rahman A, Karim MM. Green Shipbuilding and Recycling: Issues and Challenges. Int. J. Environ. Sci. Dev. 2015; 6(11): 838–842, doi: 10.7763/ijesd.2015.v6.709.

[7] Xu HL, Wang H, Xu H, Kou X, Li C, Yan HS, Du ZF, Xu WH. Discuss on green shipbuilding technology: Design and material. Adv. Mater. Res. 2012; 490–495: 3296–3300, doi: 10.4028/www.scientific.net/AMR.490-495.3296.

[8] Saputra N, Martana B, Noorohmah F, Reda R. Study on the strength of a fishing boat made from plastic Recycles. E3S Web Conf. 2021; 328: 2–6, doi: 10.1051/e3sconf/202132807002.

[9] Shaktivel MR, Prasath MA, Pragadeesh T, Hendy RS, Sriram P. Analysis of Mechanical Properties and Study of Microstructure (HDPE) Plastic Made Boat. Ind. Eng. J. 2023; 52(5): 7–13.

[10] Shanmugam V, Das O, Neisiany RE, Babu NB, Singh S, Hedenqvist MS, Berto F, Ramakrishna S. Polymer Recycling in Additive Manufacturing: an Opportunity for the Circular Economy. Mater. Circ. Econ. 2020; 2(1): 11, doi: 10.1007/s42824-020-00012-0.

[11] Cestari SP, Martin PJ, Hanna PR, Kearns MP, Mendes LC, Millar B. Use of virgin/recycled polyethylene blends in rotational moulding. J. Polym. Eng. 2021; 41(6): 509–516, doi: 10.1515/polyeng-2021-0065.

[12] Ávila AF, Duarte MV. A mechanical analysis on recycled PET/HDPE composites. Polym. Degrad. Stab. 2003; 80(2): 373–382, doi: 10.1016/S0141-3910(03)00025-9.

[13] Ozdemir T, Mengeloglu F. Some properties of composite panels made from wood flour and recycled polyethylene. Int. J. Mol. Sci. 2008; 9(12): 2559–2569, doi: 10.3390/ijms9122559.

[14] Registro Italiano Navale, RES. 22/E Rules for the classification of ships with reinforced plastic, aluminium alloy or wooden hull. 2023.
[15] RINA. Rules for the Classification of Workboats. 2020.
[16] Bureau Veritas. NR 546 - Hull in Composite,Plywood, and High Density Polyethylene Materials. 2022. https://erules.veristar.com/dy/data/bv/pdf/546-NR_2022-11.pdf.
[17] Bertagna S, Taucer Marchesi N, Bucci V, Marinò A. On the Structural Response of Innovative Plastic Materials for Boatbuilding Applications. Volume 9: Theory and Practice of Shipbuilding. 2024: 1–10, doi: 10.3233/PMST240024.
[18] Fan J, Guo X, Wu C, Crupi V, Guglielmino E. Influence of Heat Treatments on Mechanical Behavior of FV520B Steel. Exp Tech. 2015; 39(2): 55 – 64, doi: 10.1111/ext.12019.
[19] Corigliano P, Crupi V, Pei X, Dong P. DIC-based structural strain approach for low-cycle fatigue assessment of AA 5083 welded joints. Theor. Appl. Fract. Mech. 2021; 116: 103090, doi: 10.1016/j.tafmec.2021.103090.